Renewable and Sustainable Energy Reviews 14 (2010) 1860–1873

Contents lists available at ScienceDirect

Renewable and Sustainable Energy Reviews

journal homepage: www.elsevier.com/locate/rser

Using power ultrasound for the regeneration of dehumidizers in desiccant air-conditioning systems: A review of prospective studies and unexplored issues

Ye Yao [a,b,*]

[a] Institute of Refrigeration and Cryogenics, Shanghai Jiao Tong University, Shanghai 200240, China
[b] National Air Transportation Center of Excellence for Research in the Intermodal Transport Environment (RITE), School of Mechanical Engineering, Purdue University, West Lafayette, IN 47907-2031, USA

ARTICLE INFO

Article history:
Received 2 February 2010
Accepted 26 March 2010

Keywords:
Power ultrasound
Drying
Regeneration
Desiccant

ABSTRACT

Regeneration of dehumidizers is the most important stage in the working cycle of desiccant system. The lower regeneration temperature will be favorable for the energy efficiency of the whole system. Ultrasonic technology may be a promising method of dehydration applied to the regeneration of desiccant. As a non-heating method, the power ultrasonic may help lower the regeneration temperature and bring about energy savings. In the present paper, the mechanism of ultrasonic regeneration is set forth based on the ultrasonic theory as well as the mass transfer model in solid–gas and liquid–gas system. The recent studies related to ultrasonic dehydration are extensively reviewed, which is of significant reference to the study of desiccant regeneration assisted by power ultrasound. In addition, this work gives the basic ideas of ultrasonic dehydrator for solid/liquid-desiccant regeneration, which will promote the development of relevant equipments. Finally, some unexplored issues on this topic are addressed, including insight into the effects of ultrasonic on the regeneration, drying kinetics model for ultrasonic regeneration and the challenges possibly faced for the ultrasonic transducer development.

Contents

1. Introduction . . . 1860
2. Theoretical investigations . . . 1861
 2.1. Fundamental knowledge about ultrasound . . . 1861
 2.2. Mass transfer enhancement by power ultrasound . . . 1862
  2.2.1. Solid–gas mass transfer process . . . 1862
  2.2.2. Liquid–gas mass transfer process . . . 1864
3. Recent studies on ultrasonic dehydration. . . . 1865
4. Basic ideas for ultrasonic regenerator. . . . 1867
5. Related issues to further study . . . 1869
 5.1. Insight into the effects of power ultrasound on the enhancement . . . 1869
 5.2. Drying kinetics model for desiccant regeneration assisted by ultrasonic . . . 1870
 5.3. Development of ultrasonic transducer. . . . 1871
 5.4. Others . . . 1871
6. Conclusions . . . 1871
Acknowledgements . . . 1872
References . . . 1872

1. Introduction

Dehumidification is an important air-handling process in air-conditioning system, which aims at reducing the level of humidity in the air, usually for health reasons, as humid air can easily result in mildew growing inside residence and cause various health risks [1]. It is also necessary in many industrial or agricultural occasions

* Correspondence address: Institute of Refrigeration and Cryogenics, Shanghai Jiao Tong University,Dong Chuan Rd. No.800, Shanghai, 200240, China.
Tel.: +86 13641943577; fax: +86 21 34206814.
E-mail address: yeyao10000@sjtu.edu.cn.

1364-0321/$ – see front matter © 2010 Elsevier Ltd. All rights reserved.
doi:10.1016/j.rser.2010.03.042

where certain low level of air humidity is required to be maintained. Traditionally, the moist air is commonly dehumidified through refrigerant cooling method, i.e. the air is first cooled to below the dew-point temperature to condense moisture out, and then reheated to a desired temperature before it is delivered to the occupied spaces. This method not only results in additional energy dissipation due to the cooling–heating process, but also makes against the energy performance of chiller system because of the lower refrigerant evaporating temperature required. To improve the energy efficiency of the air-conditioning system, the independent humidity control system that integrates liquid/solid desiccant devices with a conventional cooling system has been developed to separate the treatment of sensible and latent load of moist air [2–4]. This system may bring about many chances of energy conservation, e.g. avoiding excess cooling and heating, utilizing waste heat rejected by machines [5] and solar energy [6] to accomplish the dehumidification. What is more, dehumidification with dehumidizers has been proved to be beneficial for improving IAQ (Indoor Air Quality) [7].

As shown in Fig. 1, the working cycle of desiccant method consists of the following three stages: (1) adsorption (from A to B); (2) regeneration or dehydration (from B to C); and (3) cooling (from C to A). During the repeated adsorption–regeneration–cooling cycle, the regeneration conditions will produce great influence on the performance of water vapor adsorption on dehumidizer [8]. Although higher regeneration temperature will contribute to increasing the desiccant volume of dehumidizer, it may be disadvantageous to the energy efficiency of desiccant system because high-temperature regeneration will not only consume large amount of thermal energy for heating the drying air, but also result in energy dissipation during the cooling process. In addition, the higher the regeneration temperature is, the more difficult it will be to utilize the low-grade energy sources widely existed in the nature. From this point of view, new types of dehumidizers [9,10] with lower regeneration temperature are attractive in this field application. In fact, the limitation of high regeneration temperature for the traditional solid desiccant may be overcome by some non-heating dehydration methods, such as pulsed corona plasma [11], pulsed vacuum [12], centrifugal forces [13], and electrical fields [14]. These non-heating methods enhance moisture transfer in materials through certain kind of physical force, and hence make it possible to apply to the drying of desiccant and lower the regeneration temperature.

Power ultrasonic is another non-heating technology that can improve the dehydration process of moist material, and becomes a promising dehydration method for desiccant regeneration [15]. Much literature [16–20] has reported that the high-intensity ultrasound can well enhance the regeneration of some adsorbents (used for water treatment), such as activated carbon and resins of different sorts (e.g. polymeric, NKA-II and CL-TBP). It is widely admitted that the regeneration enhancements attribute to some special effects (e.g. cavitation and miro-oscillation) induced by ultrasound that can overcome the affinity of the adsorbed species with the adsorbent surface and accelerate the molecular transport towards and from the adsorbent surface. The regeneration of the adsorbents for water treatment is made in solid–liquid system where the mass transfer occurs on the interface between solid and liquid. While, the desiccant regeneration usually happens in either solid–gas or liquid–gas environment. It is a brand new field for ultrasonic applications.

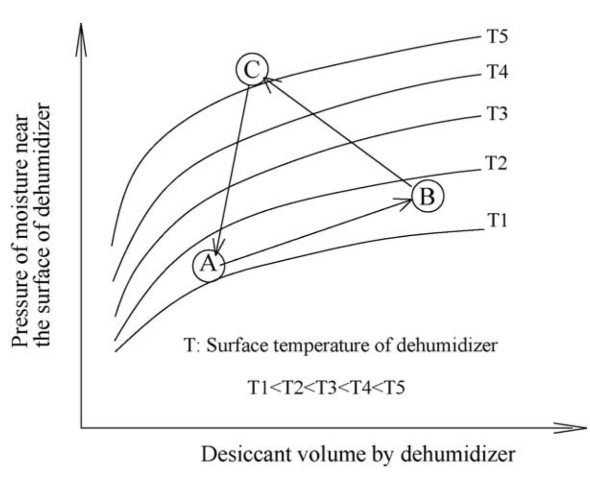


Fig. 1. Working cycle of dehumidification using dehumidizer.

The primary aims of this paper are to make clear the mechanism of mass transfer enhancement by ultrasonic in solid–gas and liquid–gas system based on an extensive review of relevant literature, and identify some unexplored issues for the future research. In order to provide a context for the main body of the review, we will begin by introducing the fundamental knowledge about ultrasound and its several special effects. Then, the mass transfer models in solid–gas and liquid–gas system are presented to illustrate the possible mechanism of enhancement by ultrasonic. Next, the recent studies on ultrasonic dehydration are summarized and reviewed. Meanwhile, some basic ideas about ultrasonic dehydrator for the regeneration of solid/liquid desiccant are put forward. Finally, some unexplored issues on the regeneration by power ultrasonic are addressed for the future study. These include the insight into the effects of ultrasonic on the improvement of desiccant regeneration, the drying kinetics model for ultrasonic regeneration, the development of ultrasonic transducer for this application and the other problems like the environmental impact and economic benefit.

2. Theoretical investigations

2.1. Fundamental knowledge about ultrasound

Sound, as a special form of energy, propagates through pressure fluctuations in elastic media. According to the frequency of pressure pulsation, sound can be classified as infrasound (lower than 20 Hz), audible sound (normally from 20 Hz to 20 kHz) and ultrasound (above 20 kHz) [21]. High-intensity ultrasound can cause some special effects, typically like cavitation, micro-oscillation and heating. The cavitation refers to the formation and subsequent dynamic behavior of vapor bubbles in liquids. It occurs when the high-intensity sound waves are coupled to the liquid surface, which results in the propagation of alternating regions of compression and expansion, and thus in the formation of micro-size vapor bubbles. If the bubbles grow up to a critical size, they may implode violently, releasing energy in the form of instant impulses with high local point temperature (attains 5000 K) and pressure (attains 1000 atm) [22]. Since the impulse time is very short (less than 0.1 s), the temperature of the bulk of the liquid hardly have a change. The micro-oscillation is due to the pressure fluctuation caused by the sound wave which makes the particles in medium alternately flex in the similar frequency of sound. Although the amplitude of vibration of the particles is very small, the acceleration may be as high as ten thousand times of the gravity [22]. The thermal effect of ultrasound can be illustrated by the following facts: on the one hand, part of ultrasonic energy is directly absorbed by medium during the transmission of ultrasonic wave; on the other hand, the oscillation caused by the sound wave intensifies the friction among particles, and ultimately converts into heat.

A system for producing ultrasound mainly consists of two parts: the generator and the transducer. The generator provides the source of energy that is converted into ultrasonic energy through the transducer. According to the phenomena involved, five main types of transducers could be considered: piezoelectric, magnetostrictive, electromagnetic, electrostatic and fluid-driven [23]. The piezoelectric transducers produce acoustic energy by changes in size produced by electrical signals in piezoceramic materials (such as quartz, tourmaline and zinc oxide). The magnetostrictive transducer is made from certain metal, such as nickel, cobalt and iron, which changes in dimension upon the application of a magnetic field. The repeated changes of physical size produce mechanical vibrations. The electromagnetic transducer is made from a solid armature (e.g. membrane in loudspeaker and microphones) that produces vibration due to coupled electric and magnetic field. The electrostatic transducer generates mechanical vibration through the periodic variation of charges in an electrical capacitor of special design. And the fluid-driven transducer produces acoustic waves when the kinetic energy of a fluid makes a mobile part of a system vibrate. Among these transducers, the piezoelectric are most commonly used to generate high-intensity ultrasound (ranging from 15 kHz to 10 GHz) for experimental studies related to power ultrasound applications.

When the sound source can be considered as a point source in a free space, and the sound intensity decreases inversely with the square of the distance from the point source. However, the ultrasonic transducers are usually shaped as horn, paraboloid or ellipsoid. The sound radiation can be regarded as coming from a plane source. According to the Huygens–Fresnel principle [24], the pattern of sound intensity distribution can be schematically illustrated as shown in Fig. 2. The sound intensity is constant within the zone near the sound source (called the Fresnel zone), whereas outside this zone (called the Fraunhofer zone), the sound intensity decreases in the same way as for a point source. The length of the near zone, L, can be approximately determined by Eq. (1):

$$L = \frac{d^2}{4\lambda} = \frac{d^2 f}{4V} \tag{1}$$

where d is the diameter of sound plate, m; λ is sound wavelength, m; f is sound frequency, Hz; V is sound velocity, m/s.

All of the energy of the wave in the Fraunhofer zone is concentrated in a cone whose divergence angle, a, is determined by:

$$a = \sin^{-1}\left(\frac{K \cdot \lambda}{d}\right) = \sin^{-1}\left(\frac{K \cdot V}{d \cdot f}\right) \tag{2}$$

where K is a constant which depends on the following factors: the edge of the beam (or the beam boundary); the shape of the transducer, i.e. whether circular or rectangular; and the method used to determine beam spread, i.e. the pulse echo method or the transmission method [25].

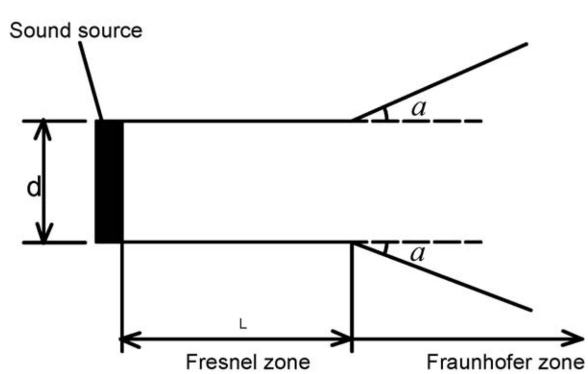


Fig. 2. Propagation pattern from a plane sound source.

Known from Eqs. (1) and (2), sound frequency is the key parameter that influences both the Fresnel zone length and the divergence angle in Fraunhofer zone. In any case, the length of the Fresnel zone will increase and the angle of divergence will decrease as the sound frequency increases. In some configurations of the power ultrasonic transducers for industrial use, the length of zones and thus sound intensity distribution may become important. For example, in the gaseous medium, the Fresnel zone for the plane source with 10 cm in diameter is negligible (less than 1 mm) for sound at 100 Hz, but extends for about 16 cm when the acoustic frequency arrives at 20 kHz, which greatly expands the scales of interest of ultrasound in drying or dewatering applications (e.g. the regeneration of dehumidizers).

In the case of a plane progressive wave penetrating the material being dried, the sound energy is damped due to various mechanisms including relaxation, viscous shearing effects and molecular absorption. In porous medium, the frame parameters (e.g. porosity, pore shape and permeability) and the viscous action of the fluid motion relative to the frame as well as the acoustic parameters (frequency and wave velocity) are usually taken into account to determine the acoustic attenuation coefficient (δ) [26]:

$$\delta = \left(\frac{f \nu \varphi \gamma s_{\rm p}^2}{\pi \kappa_{\rm o} V^2}\right)^{1/2} \tag{3}$$

where γ is the specific heat ratio of fluid in porous medium; ϕ is porosity; $s_{\rm p}$ is pore shape factor; $\kappa_{\rm o}$ is the static permeability of porous medium; ν is the kinematic viscosity of fluid in porous medium.

Neglecting the scattering of sound energy, the sound intensity at a distance of x from the material surface at which the incident sound intensity is $I_{\rm o}$ can be calculated by:

$$I(D) = I_{\rm o}\exp(-2\delta x) \tag{4}$$

Eq. (3) makes clear that the attenuation coefficient is proportional to the square-root of frequency, which indicates the higher frequency in sound will lead to the faster energy damping in medium and thus the effective zone where the sound energy is above a certain threshold value will be dwindled. Hence, the choice of frequency is extremely crucial for the highly efficient use of ultrasonic energy in drying or dewatering process.

2.2. Mass transfer enhancement by power ultrasound

As mentioned above, high-intensity ultrasound produces a variety of effects, such as micro-oscillating, cavitation, streaming, and radiation heating. These effects can influence mass transfer processes by producing changes in concentration gradients, diffusion coefficients, or boundary layer. The effects may be very different for different physical states of system. According to the type of dehumidizers used in desiccant air-conditioning system, the regeneration process can be classified as the solid–gas and liquid–gas mass transfer processes.

2.2.1. Solid–gas mass transfer process

The solid–gas mass transfer process usually occurs in the solid desiccant system. The microporous solids such as silica gels and molecular sieves are often served for dehumidizers. To probe into the mechanism of mass transfer enhancement assisted by power ultrasound in solid–gas system, the moisture transport in silica gel is illustrated here.

Silica gel has very high moisture adsorption capacity because of its microporous structure of internal interlocking cavities that is of

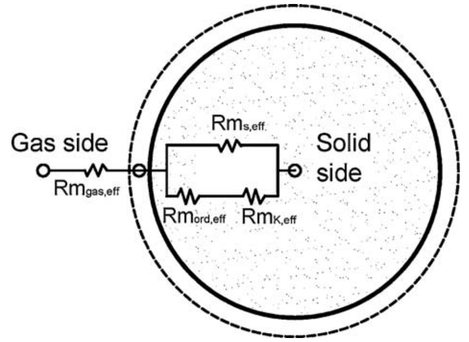


Fig. 3. Detailed resistance model of mass transfer for silica gel.

a high internal surface area up to 800 m^2/g [27]. During the regeneration, the water vapor pressure in the drying air is normally lower than that at or near the external surface of the silica gel particles. Such kind of pressure difference drives the water molecules in silica gel diffuse to the surface, and then enter into the air. So, the mass transport should have two basic processes: the first is moisture diffusion in silica gel (solid-side mass transfer); another is convective mass transfer between silica gel surface and air (gas-side mass transfer). The schematic representation for the resistance model of mass transfer for silica gel is shown in Fig. 3. The total mass transfer coefficient (K_{total}: kg/m^2 s) including the solid-side ($K_{m,solid}$: kg/m^2 s) and the gas-side ($K_{m,gas}$: kg/m^2 s) can be integrated as:

$$K_{total} = \left(\frac{1}{K_{m,soild}} + \frac{1}{K_{m,gas}}\right)^{-1} \tag{5}$$

2.2.1.1. Solid-side. As shown in Fig. 2, the three main transport mechanisms on solid-side are the ordinary, Knudsen and surface diffusion. The ordinary diffusion occurs when the molecules of the gas collide with each other more often than with the pore walls of a porous medium, and the Knudsen diffusion occurs when the gas molecules collide more frequently with pore walls than with each other [28]. For water vapor–air mixtures, the ordinary diffusion coefficient (D_{ord}: m^2/s) and the Knudsen coefficient (D_K: m^2/s) can be written, respectively, by Eqs. (6) and (7) [29].

$$D_{ord} = 1.735 \times 10^{-9} \frac{(t + 273.15)^{1.685}}{P_w} \tag{6}$$

$$D_K = 22.86 \times (t + 273.15)^{0.5} \cdot r_{pore} \tag{7}$$

where t is the gas temperature, °C; P_w is the water vapor pressure, atm; r_{pore} is average pore radius, m.

The pore void diffusion coefficient (D_{void}: m^2/s) then may be approximately represented by an addictive resistance based on the ordinary and the Knudsen coefficient [29]:

$$D_{void} = \left[\frac{1}{D_{ord}} + \frac{1}{D_K}\right]^{-1} \tag{8}$$

Eqs. (6)–(8) are valid only for long, uniform radius capillaries. For real porous medium, the pore void diffusion coefficient should be modified as [30]:

$$D_{void,eff} = \frac{\varepsilon_p}{\tau_g} D_{void} \tag{9}$$

where $D_{void,eff}$ is called the effective pore void diffusion coefficient, m^2/s; ε_p is particle porosity which accounts for the reduction of free area for diffusion due to presence of solid phase; τ_g stands for gas tortuosity factor that accounts for the increase in diffusion length due to tortuous paths of real pores.

The surface diffusion is the transport of adsorbed molecules on the pore. The main mechanisms to explain surface flow include the hopping model, which takes into account that the gas molecules move on the surface by jumping from site to site with a specific velocity [31]. Based on the mechanistic hopping model, the expression (Eq. (10)) for the effective surface diffusion coefficient ($D_{s,eff}$: m^2/s) was obtained by Sladek et al. [32].

$$D_{s,eff} = \frac{1.6 \times 10^{-6}}{\tau_s} \exp\left(\frac{-0.974 H_{ads}}{t + 273.15}\right) \tag{10}$$

where τ_s is surface tortuosity factor that accounts for the increase in diffusion length due to tortuous paths of real pores; H_{ads} is the heat of adsorption (kJ/kg), which may be considered as a function of moisture ratio (W, kg water/(kg dry sample)) in solid desiccant. For regular density silica gel with certain moisture ratio, H_{ads} may be experimentally given by [33]:

$$H_{ads} = -1400W + 2950, \quad W > 0.05 \tag{11}$$

Since the pore void diffusion and the surface diffusion are parallel process, the total diffusivity in solid-side (D_{solid}: m^2/s) can be written as:

$$D_{solid} = D_{s,eff} + \frac{g'}{\rho_p} D_{void,eff} \tag{12}$$

where ρ_p is particle density, kg/m^3; g' is derivative of equilibrium isotherm, kg/m^3, varying from 0 to 0.4 for regular density silica gel [30].

The lumped parameter model for the solid-side mass transfer coefficient ($K_{m,solid}$: kg/m^2 s) may be expressed as:

$$K_{m,solid} = \frac{\rho_p D_{solid}}{r_p} \tag{13}$$

where r_p is the particle radius, m.

Known from Eqs. (6) through (12), the factors that influence the solid-side diffusivity in porous medium mainly include the pore size, the pressure, the temperature and the moisture ratio. Using the data published in literature [33], these influential factors are plotted in Figs. 3 and 4, respectively. The basic calculation parameters include: $r_p = 2 \times 10^{-3}$ m; $\rho_p = 721.1$ kg/m^3; $\tau_g = \tau_s = 2.8$; $\varepsilon_p = 0.716$; $g' = 0.2$.

It can be seen from Fig. 4 that the water vapor pressure in porous medium has little influence on the solid-side diffusivity when the pore size is smaller than 200 Å. So, for those microporous solid desiccants like silica gel whose pore size is no bigger than 100 Å, the contribution of 'micro-oscillation effect' of power ultrasound to the solid-side diffusivity may be negligible. However, for those macroporous medium like green rice whose

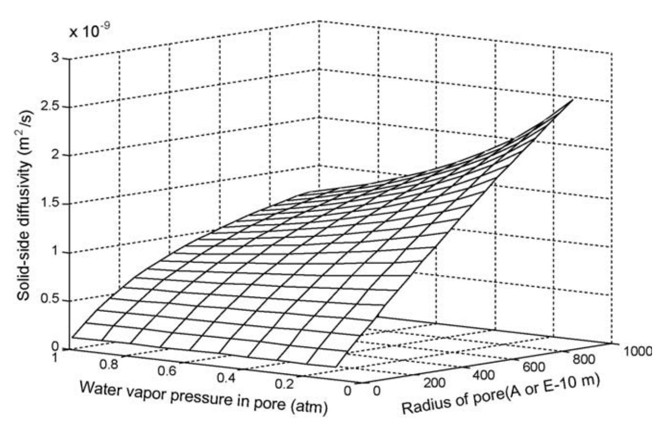


Fig. 4. Effect of pore size and water vapor pressure in pore on the solid-side diffusivity (t = 40 °C).

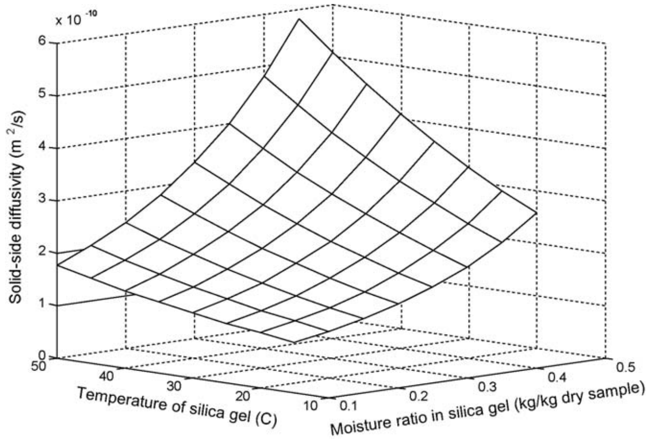


Fig. 5. Effect of body temperature and moisture ratio on the solid-side diffusivity (r_{pore} = 20 Å, P_w = 1.0 atm).

pore size may be larger than 1000 Å, the micro-oscillation effect that induces a series of pulsation partial vacuum in the medium (which equals to lowering the water vapor pressure) may affect the water vapor transport [34]. As shown in Fig. 3, the influence of water vapor pressure on the diffusivity becomes important as the pore radius attains 1000 Å.

Fig. 5 shows that both the temperature and the moisture ratio of the solid medium produce great impact on the solid-side diffusivity which will increase with the two factors. The influence of the temperature on the diffusivity becomes more significant under a higher moisture ratio in silica gel. As the sonic energy is dissipated as heat and make the material temperature increase, the thermal effect of power ultrasonic is sure to improve the moisture transport in porous medium.

2.2.1.2. Gas-side. The gas-side mass transfer coefficient ($K_{m,gas}$: kg/ m^2 s) may be defined as:

$$K_{m,gas} = \frac{\rho_{gas} D_{gas}}{\delta} \tag{14}$$

where ρ_{gas} is the gas (dry air + water vapor) density, kg/m^3; D_{gas} is the gas-side diffusivity, m^2/s; δ is the thickness of particle surface layer where there is a gradient of moisture concentration. In literature [35], $K_{m,gas}$ is empirically related to the air flow rate passing by the particles:

$$K_{m,gas} = 0.704 G_{gas} Re^{-0.51} \tag{15}$$

where Re = $(U_D r_p)/\nu_{gas}$; G_{gas} is air mass flow rate per unit area of porous medium, =$(\rho_{gas} V_{gas} A_c / A_s)$, kg/m^2 s; V_{gas} is upstream velocity before porous medium, m/s; A_c is cross-sectional area of upstream, m^2; A_s is total external area of porous medium, m^2; ν_{gas} is kinematic viscosity of gas in porous medium, m^2/s; U_D is Darcy velocity, m/s, =V_{gas}/ε_V; ε_V is the volume fraction of gas in porous medium, which can be computed according to the packing angle θ [36]:

$$\varepsilon_V = 1 - \frac{\pi}{6(1 - \cos\theta)\sqrt{1 + 2\cos\theta}} \tag{16}$$

Eq. (16) is only valid for packing angles between 60° and 90° (resulting in computed ε_V between 0.2595 and 0.4764).

Since D_{gas} is mainly affected by the difference of moisture concentration between the particle surface and the gaseous phase, the increase in the gas-side mass transfer coefficient ($K_{m,gas}$) brought by the increase of air mass flow rate (G_a) (Eq. (14)) may, to a large extent, owe to the reduction of the thickness of the laminar sub-layer surrounding the particle (δ) because of the increased gas velocity. The effect of micro-oscillation induced by power ultrasound may have a similar result of increasing the air mass flow rate, which intensifies the turbulence of gas stream flowing over the material and reduces the thickness of the boundary layer. It is reported that a substantial decrease (up to 15%) in the boundary layer thickness may be achieved by high-intensity sound with 15 kHz and 155 dB during the drying process [23]. The gas-side mass transfer enhancement by power ultrasound may be explained as well by the theory of acoustic streaming [37]. The acoustic streaming is a steady circular air flow occurring in a high-intensity sound field, which is attributed to the friction between a fluid medium and a vibrating object. So, when the solid is vibrated by the high-intensity ultrasound, there will be an oscillation tangential relative velocity between the solid surface and the fluid passing by, which is especially effective in promoting certain kinds of rate process occurring on the solid and fluid interface including the heat and mass transfer [38].

The analysis above indicates the following possible mechanisms of mass transfer enhancement in a solid–gas system by power ultrasound:

(1) For microporous materials (like silica gel and molecular sieves) whose pore sizes are normally smaller than 200 Å, the sound waves enhance the moisture diffusivity inside medium mainly due to temperature rise caused by its thermal effect. But for macroporous materials with pore size larger than 200 Å, the effect of an ultrasound field on the solid-side moisture diffusivity may be both thermal and mechanical.
(2) The gas-side mass transfer alteration mainly owes to the mechanical effect of power ultrasound that causes oscillating velocities and micro-streaming at solid/gas interfaces which may affect the diffusion boundary layer.

2.2.2. Liquid–gas mass transfer process

In liquid environment, the ultrasound with certain intensity and frequency can induce 'cavitation' in which a great number of micro-size vapor bubbles are formed and subsequently implode violently. As the bubbles implode at or near the surface of liquid, fine liquid droplets can be released into the surrounding air and evaporated instantaneously. This phenomenon is called as ultrasonic atomization. The diameter of droplet (d_m, m) ultrasonically atomized may be theoretically calculated by [39]:

$$d_m = 2.8\left[\frac{\sigma_s}{\rho_s f^2}\right]^{1/3}\left(\frac{\mu_s}{\mu_w}\right)^{-0.18} \tag{17}$$

where σ_s is surface tension in solution, N/m; ρ_s is solution density, kg/m^3; μ_s and μ_w is the viscosity of bulk solution and water, respectively, Pa s. When the ultrasonic frequency (f) attains 2.0 MHz, the diameter of droplets can be as small as several microns.

In liquid–gas system, the mass transfer process can be surely enhanced when the liquid is atomized and dispersed into the gaseous phase. Under the lower Reynolds Number (Re $<$ 400), the mass transfer coefficient of liquid droplet ($K_{m,ld}$: m/s) may be calculated by using the following empirical equation [40]:

$$K_{m,ld} = \frac{D}{d_{ld}}\left(1 + \left(Sc + \frac{1}{Re}\right)^{1/3} Re^{0.41}\right) \tag{18}$$

where D is molecular diffusivity in continuous phase (gaseous phase), m^2/s; d_{ld} is diameter of liquid droplet, m; Re is Reynolds number, =$U_a d_{ld}/\nu_a$; U_a is velocity of streaming air, m/s; ν_a is kinematic viscosity, m^2/s; Sc Schmidt number, =ν_a/D.

Fig. 5 shows the effect of droplet size on the mass transfer coefficient of a LiBr solution droplet exposed to an airstream at 40 °C. The molecular diffusivity (D) is approximated as 1.005×10^{-9} m^2/s according to literature [41], and the air kinematic viscosity ν_a = 17.65×10^{-6} m^2/s in the calculation. As

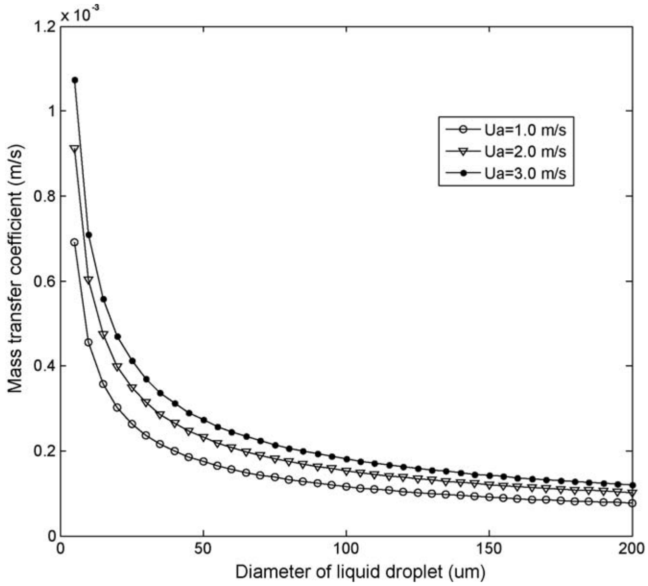


Fig. 6. Mass transfer coefficients for a liquid sphere in free streaming of air at 40 °C.

illustrated in Fig. 6, the water evaporation rate in LiBr solution increases greatly with the decrease of the droplet size, especially within the range of 0–50 μm in the droplet diameter.

3. Recent studies on ultrasonic dehydration

This part will review the relevant literature about ultrasonic dehydration under the solid–gas and liquid–gas circumstances.

Drying the fruits, vegetables and other plant tissues is an example of mass transfer from the solid medium to the gas medium. Gallego-Juarez et al. [42] made an experimental study about the use of high-intensity ultrasound for vegetable dehydration by using a special power ultrasound generator with a stepped plate that has a direct contact with the product. The ultrasonic frequency employed in their experiments is about 20 kHz. The results show that by using the power ultrasound it is possible to reduce dramatically the treatment time and it is relatively easier to reach a target moisture content (less than 1%) in the samples. In addition, the authors announced that their new ultrasonic system would be highlighted by its favorable energy utilization efficiency in food dehydration applications when compared to the conventional hot-air drying procedure. Based on the data published in literature [43], Mulet et al. [44] calculated the effective water diffusivity in carrot under different drying temperatures combined with or without ultrasound using the diffusive model for carrots proposed by his previous work [45]. Although the model did not consider the external resistance to mass transfer and other actual complex conditions, the obtained results were still valid to prove that under similar conditions (e.g. air velocity is 1.3 m/s, drying temperature is 60 °C) the carrot diffusivity in experiments carried out with ultrasound (about 0.74 E−9 m^2/s) was obviously higher than that without ultrasound (about 1.35 E−9 m^2/s). In addition, the results showed that the relative influence of ultrasound on the drying decreased when the drying air temperature increased. When the drying temperature rose to 90 °C, the diffusivity under the similar-power ultrasound was only about 0.38 E−9 m^2/s higher than that without ultrasonic radiation (2.15 E−9 m^2/s). Especially, when the air temperature arrived at 115 °C, hardly no differences in diffusivity were found between applying and not applying ultrasound. In another work by Carcia-Perez et al. [46], drying kinetics of carrot cubes were carried out at 1 m/s air velocity at different air drying temperatures (30, 40, 50, 60 and 70 ± 0.1 °C)

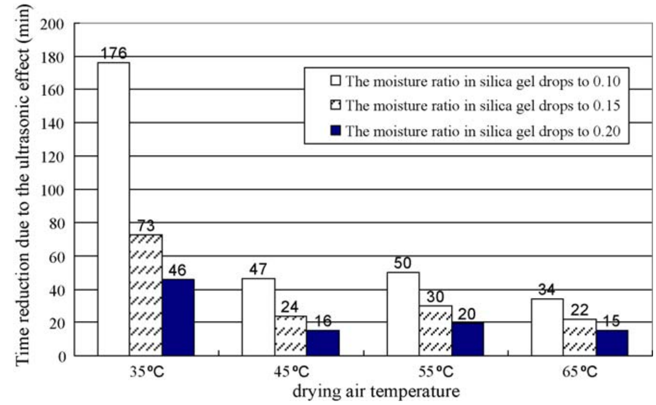


Fig. 7. Comparisons of drying time reduction due to the ultrasonic radiation under different drying temperatures.

by applying and not applying high-power ultrasound. The experimental results showed that ultrasound did increase the drying rate at different temperatures, but the improvement on drying rate decreased at high temperatures, and almost disappeared at 70 °C. Similar effects were also found by Yao et al. [47] when applying the same technique to drying silica gel (a kind of porous material for air dehumidifying). The application of a high-power ultrasonic (25.6 kHz, 40 W) vibration in direct contact with wet silica gel samples has improved the kinetics of dehydration (the process of regeneration) as compared to non-ultrasonic radiation. However, the improvement tends to decrease with the rising of the air temperature, which can be reflected from Fig. 7 by comparing the reduced drying (regeneration) time due to the ultrasound for the same dehydration quantity (i.e. from the identical initial moisture ratio to the target ratio) under different drying air temperatures. This behavior may be explained by the following two reasons. First, the air temperature may disturb the acoustic field in porous medium. The study by Jakevicius and Demcenko [48] manifests that the acoustic attenuation will increase with increasing air temperatures when the ultrasound ($f < 200$ kHz) propagates in a closed chamber. It indicates that the higher air temperature may result in more energy dissipation of ultrasound and reducing the energy present in the medium, and hence, degrade the ultrasonic effects. Secondly, the higher temperature is adverse to the working efficiency of ultrasonic transducer. The electromechanical coupling factor of the piezoelectric material (the key factor impacting the efficiency of ultrasonic transducer) has been proved to inversely increase with the temperature (see Fig. 8) [49].

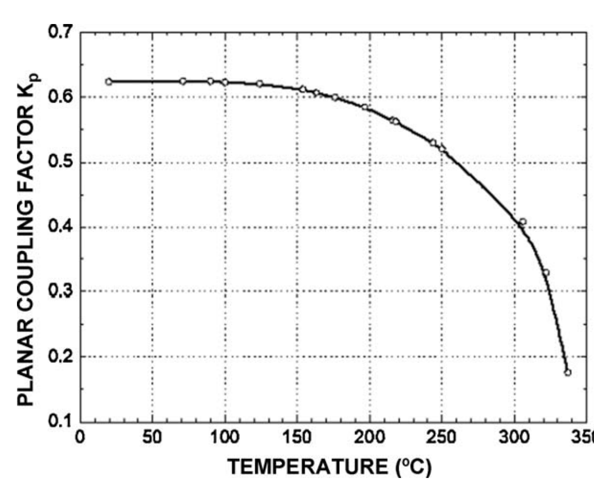


Fig. 8. Effect of temperature on the electromechanical planar coupling coefficient between room temperature and the Curie point [49].

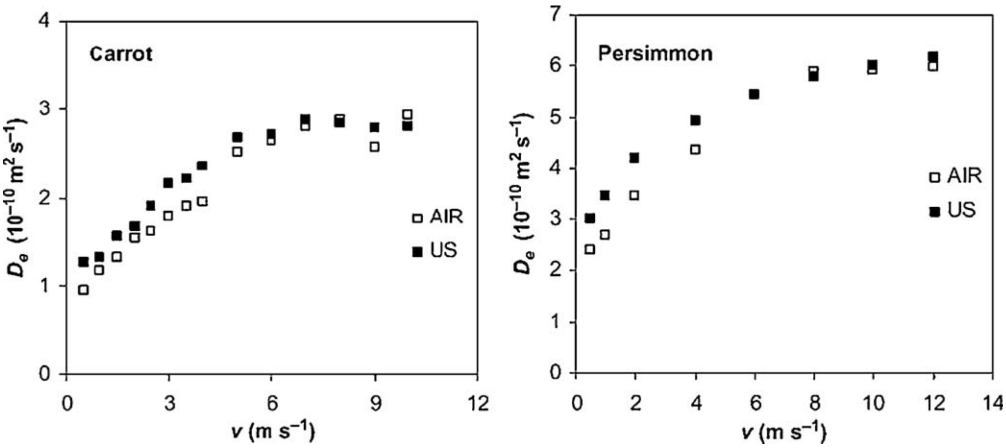


Fig. 9. Effect of air flow rate on the moisture diffusivity in carrot and persimmon with and without ultrasound (US: with ultrasound; AIR: without ultrasound) [51].

Besides air temperature, the air velocity will impact the effect of power ultrasonic dehydration. In the work by Garcia-Perez et al. [50], the effect of air flow rate (in the range of 0.6–10 m/s) on the ultrasonic drying of carrot cubes is studied. The result indicates that the power ultrasound (about 21.8 kHz) with 75 W increases the drying rate greatly at low air velocity (0.6 m/s), but when the air velocity exceeds 5 m/s, the effect of ultrasound on the drying kinetics becomes negligible. In their another publication [51], the influence of air flow rate on the ultrasound effects (21.8 kHz, 75 W) in drying process is observed for carrot and persimmon. The mass diffusivities were obtained by different diffusion models according to the geometry, which are given by Fig. 9. It shows that the improvement of moisture diffusivity brought by the ultrasound has an obvious decrease as the air velocity increases. When the air velocity exceeds 6 m/s, the improvement is negligible. To explain the trend affect of air flow rate, the total mass transfer coefficient in solid–gas system is simulated. As depicted in Section 2.2.1, two resistances are related to the mass transfer: the solid-side (internal resistance) and the gas-side (external resistance). Taking the silica gel for example, the effects air flow rate on the total mass transfer coefficients (using Eqs. (5)–(15)) are shown in Fig. 10. The basic calculation parameters include: $r_p = 2 \times 10^{-3}$ m; $\rho_p = 721.1$ kg/m^3; $\tau_g = \tau_s = 2.8$; $\varepsilon_p = 0.716$; $g' = 0.2$; $P_w = 1$ atm; $W = 0.3$ kg water/(kg dry sample); $A_c = 0.01$ m^2; $A_s = 0.2912$ m^2; $\rho_{gas} = 1.05$ kg/m^3; $\nu_{gas} = 16.4$ E−06 m^2/s; $\varepsilon_V = 0.35$. As seen from Fig. 10, influence of air flow rate on the mass transfer becomes small at the high-value region, which indicates that internal resistance become dominating in the total mass transfer at high air velocity. The power ultrasound impacts on the internal mass transfer resistance of silica gel primarily through the thermal effect, and on the external resistance through the mechanical oscillation. It is reasonable to assume that power ultrasound mainly affect external resistance to mass transfer because the temperature rise in the material due to ultrasonic thermal effect is only in the order of a few degrees [22]. This has been illustrated by Yao's study [52] which showed that the ultrasound with 40 W in power could only cause a small increase (not more than 2 °C) in the surface temperature of silica gel, but the enhancement of regeneration was equivalent to increasing the drying air temperature by 10 °C. For this reason ultrasound influence will become very small at high air velocities in which the mass transfer would be controlled by internal resistance.

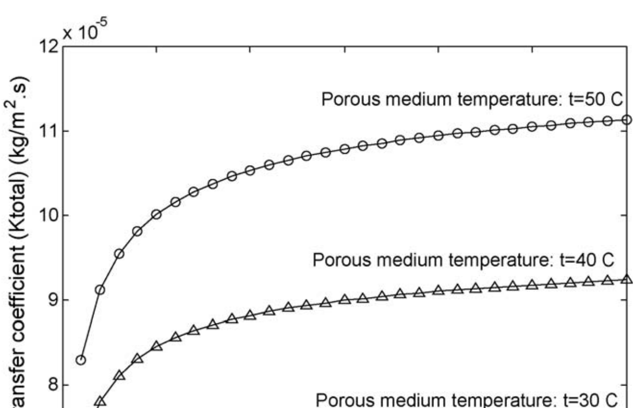


Fig. 10. Effect of air flow rate on the total mass transfer coefficients of silica gel.

In liquid–gas environment, the mass transfer enhancement can be achieved through ultrasonic atomization because the finer the droplet size is, the more rapid the evaporation will be. The technology of ultrasonic atomization has been used to assist the dehydration process of pure liquids or solutions. The selective separation of ethanol from ethanol–water mixtures by ultrasonic atomization has been reported by Sato et al. [53]. In that work, experimental data were reported that pure ethanol could be obtained directly from a solution with several mol% ethanol–water solution at 10 °C. The authors (Sato et al.) explained the fact using the mechanism of capillary wave formation that is analogous to the capillary hypothesis with the additional premise that selective separation pattern is a result of parametric decay or down conversion of an ultrasonic wave. However, they could not provide a clear explanation for the elective separation of ethanol or detect the capillary wave patterns. Kirpalani and Toll [54] gave a physical explanation for the ultrasonic separation of alcohol–water mixtures. They thought that the selective separation of alcohols could be explained as an effect of the micro-bubbles induced by the high-intensity ultrasound, i.e. the alcohol molecules vaporize into the micro-bubbles and release an alcohol-rich mist on their collapse in regions of high accumulation of acoustic energy. This explanation is still dissatisfying because no test data in this experimental study have proved the high-concentration of alcohol in the micro-bubbles. Experiments in this work found an obvious decrease in ethanol concentration in the falling liquid droplets, while the bulk liquid did not have a marked decrease until after 15 min. So, the authors supposed that the separation did not occur

at the entire liquid surface but only in the fountain jet formed by ultrasound. Strictly, there should still be separation process taking place at the liquid–gas interface of the bulk liquid because the evaporation process cannot cease under such circumstance. Just because the evaporation rate was very small, it made little influence on the bulk liquid concentration. However, the ethanol concentration could be visibly observed to decrease in the falling liquid droplets. The contrast can actually prove that the ultrasonic atomization can greatly increase the evaporation rate of solution due to the enhanced mass transfer indicated by Eq. (18). The technology is also used to dry some slurry food. Taylor and Hansen [55] have developed special ultrasonic atomizers (i.e. API-style and screen-style) which have been validated to be effective for the dehydration of dilute solutions, thus suggesting ultrasonic drying may be used as an alternative to spray drying. In their ultrasonic dryer system developed, the foodstuff liquid is first atomized to produce small-diameter droplets through the cavitation effect of power ultrasound, and then the food particles are subjected to heating to remove the water.

The ultrasonic effects in mass transfer processes are influenced by both the intensity and frequency. Intensity is directly related to the energy applied. In order to utilize ultrasonic energy more efficiently, it is necessary to investigate the influence of intensity on the effects of drying process. Garcia-Perez et al. [56] made an experimental study on the convective drying of carrot and lemon peel by applying ultrasound (21.7 kHz) with different levels of acoustic power density (0, 4, 8, 12, 16, 21, 25, 29, 33 and 37 kW/m^3). The effective moisture diffusivities of carrot and lemon peel under different levels of acoustic energy were obtained by this study (see Fig. 11). It shows that the higher intensity in ultrasonic power results in a higher moisture diffusivity in lemon peel. But for carrot, there appears to be a threshold of intensity (about 12 kW/m^3) above which the ultrasonic effects on the moisture diffusivity can become significant. Yao et al. [57] have investigated the moisture diffusivity in silica gel (initial moisture ratio is about 0.33) with and without ultrasound under different drying air temperatures. Fig. 12 shows the influence of acoustic power intensity (f = 26 kHz) on the moisture diffusivity in silica gel. As seen from Fig. 12, the moisture diffusivity increases with increasing power intensity of the ultrasound. The energy-saving rates brought by ultrasound (f = 21 kHz) with different power intensities were also analyzed. The results (see Fig. 13) indicate that within the range from 0 to 60 W, the higher ultrasonic power tends to result in the higher energy-saving rate (ESR) in silica gel regeneration. The ESR brought by ultrasound may be influenced by other factors, e.g. the drying air temperature. As shown in Fig. 13, the ESR drops as the drying air temperature increases.

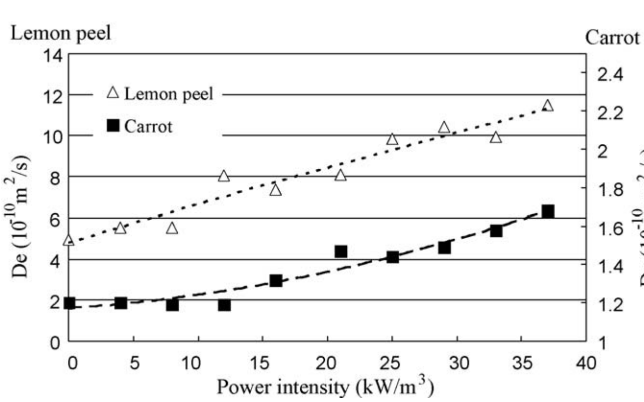


Fig. 11. Influence of acoustic power density on effective moisture diffusivity for carrot and lemon peel drying (drying air temperature: 40 °C; air velocity: 1.0 m/s).

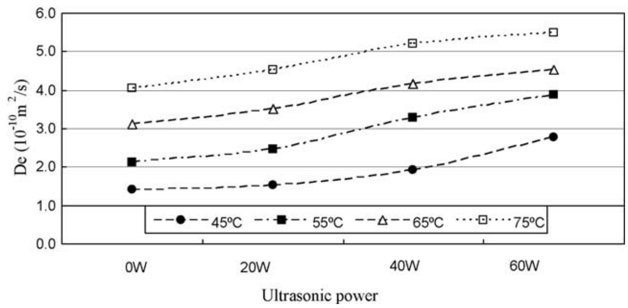


Fig. 12. Influence of acoustic power density on effective moisture diffusivity of silica gel drying (acoustic frequency: 26 kHz; mass of dry sample: 150.8 g; air mass flow rate: 3.1×10^{-4} kg/s).

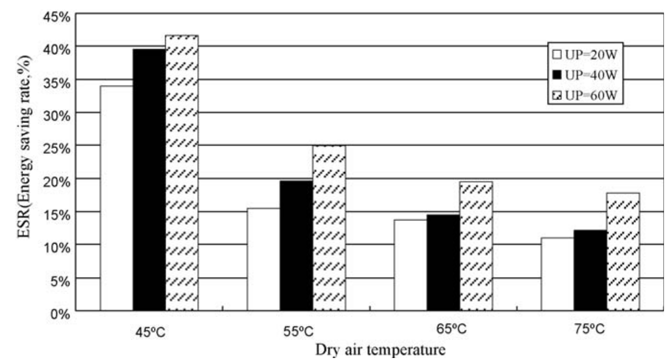


Fig. 13. Energy-saving rates by applying ultrasound with different power intensity (acoustic frequency: 21 kHz; regeneration degree: 0.3).

Frequency is another important parameter for ultrasound applications. Jambrak et al. [58] compared the treatments of vegetables by high-intensity ultrasound with 20 kHz and 40 kHz in frequency. It was found that the treatment with 20 kHz would be obviously better than that with 40 kHz. In Yao's study [58], the influence of acoustic frequency on silica gel regeneration assisted by ultrasound was investigated. The results of moisture diffusivity in silica gel versus the ultrasonic frequency are plotted in Fig. 14. It indicates that the ultrasound with a lower frequency will be favorable for the improvement of moisture diffusivity in silica gel. This may be explained by the attenuation equation of sound (Eq. (3)) which manifests that the higher frequency results in more energy dissipation in porous medium and, as a result, the ultrasonic effects on the silica gel regeneration are to be weakened.

4. Basic ideas for ultrasonic regenerator

Fig. 15 gives the basic idea of rotary desiccant regenerator assisted by power ultrasound [59]. As seen from the N–N side view,

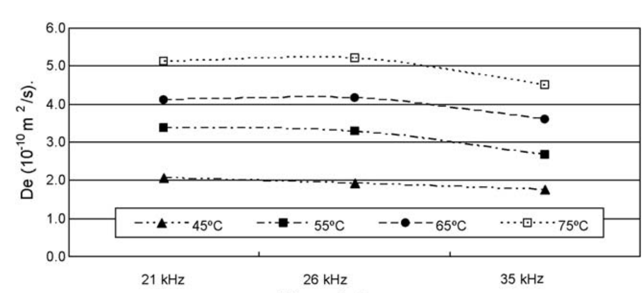


Fig. 14. Influence of acoustic frequency on effective moisture diffusivity of silica gel drying (acoustic power: 40 W; mass of dry sample: 150.8 g; air mass flow rate: 3.1×10^{-4} kg/s).

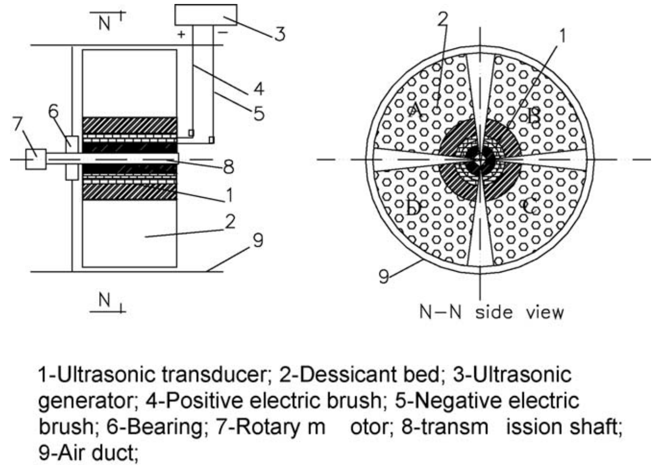


Fig. 15. Schematic diagram of rotary desiccant regenerator assisted by high-intensity ultrasound. (1) Ultrasonic transducer; (2) dessicant bed; (3) ultrasonic generator; (4) positive electric brush; (5) negative electric brush; (6) bearing; (7) rotary motor; (8) transmission shaft; (9) air duct.

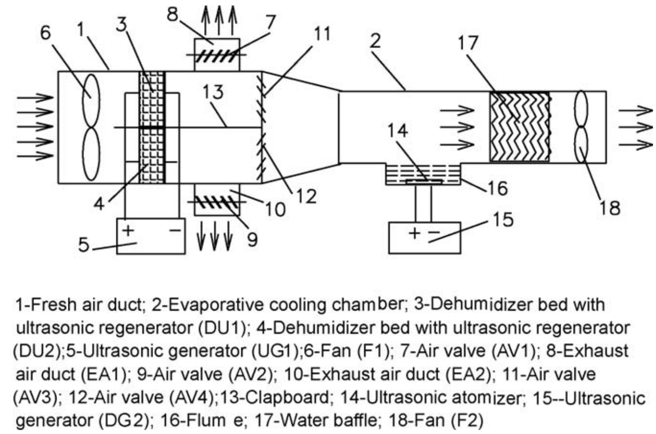


Fig. 17. Evaporative cooling system based on ultrasonic technology. (1) fresh air duct; (2) evaporative cooling chamber; (3) dehumidizer bed with ultrasonic regenerator (DU1); (4) dehumidizer bed with ultrasonic regenerator (DU2); (5) ultrasonic generator (UG1); (6) fan (F1); (7) air valve (AV1); (8) exhaust air duct (EA1); (9) air valve (AV2); (10) exhaust air duct (EA2); (11) air valve (AV3); (12) air valve (AV4); (13) clapboard; (14) ultrasonic atomizer; (15) ultrasonic generator (DG2); (16) flume; (17) water baffle; (18) fan (F2).

the regenerator consists of four individual parts each of which is made of a desiccant bed and an ultrasonic transducer. The desiccant bed is used for desiccant stuffing. Its side face is opened with numerous orifices, whose size should be smaller than the desiccant particles, for air passing. The ultrasonic transducer is designed as a shape of camber (see Fig. 16 for detail). So, the piezoelectric ceramics used in the transducer is of arc shape whose center angle is about 85°. When the rotary desiccant regenerator is applied in the desiccant system, the cross-section of its air channel is divided into two zones by clapboard: one (about 1/4 of the cross-section area) for desiccant regeneration, the other (about 3/4 of the cross-section area) for air dehumidification. The regenerator is driven by the motor to rotate discontinuously with certain periodical time. The rotary angle is set as 1/4 circle for each time so that one of the ultrasonic transducers can be connected with the ultrasonic generator and start to work for the desiccant regeneration, while the other transducers stop working and the corresponding subsections are used for air dehumidification.

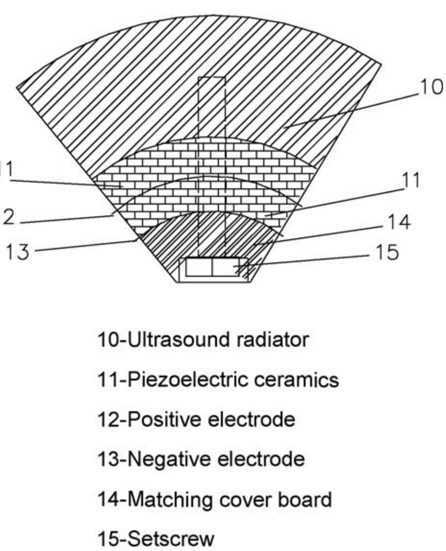


Fig. 16. Ultrasonic transducer in the rotary desiccant regenerator. (10) Ultrasound radiator; (11) piezoelectric ceramics; (12) positive electrode; (13) negative electrode; (14) matching cover board; (15) set screw.

Evaporative cooling systems used to lower the temperature of air by using latent heat of evaporation, changing water to vapor. Such kind of system has some highlighted advantages, such as simplicity of operation, low initial and maintenance costs, 100% fresh air and favorable energy-saving performance. But, it is only suitable for hot regions of low to moderate humidity [60]. If we want to extend its application to the hot and high-humidity regions, the fresh air must be firstly dehumidified in advance, and then be cooled through evaporation. Fig. 17 provides the basic idea for a kind of evaporative cooler using the ultrasonic technology [61]. The key components in this system include the two-dehumidizer beds with ultrasonic regenerators (DU1 and DU2) and one ultrasonic atomizer. The basic structure of the ultrasonic regenerator is shown in Fig. 18. The two ultrasonic regenerators operate by turns. For example, when the ultrasonic transducer in DU1 is running to dry the desiccant (regeneration process), the other in DU2 will stop working and the corresponding desiccant begins to dehumidify the fresh air. In such case, the air valve (AV1) and the air valve (AV4) is on, and the air valve (AV2) and the air valve (AV3) is off. Part of the intake fresh air passes through DU1 and exhausts outside, taking away the moisture in the desiccant assisted by ultrasonic energy. The rest of the fresh air passes through DU2, being first dehumidified, then enters into the evaporative cooling chamber in which it is cooled by numerous water droplets (10–50 μm in size produced by the ultrasonic atomizer) through water evaporation, and finally is sent to the air-conditioned space. To improve the working efficiency of the system, the fresh air for the desiccant regeneration should be

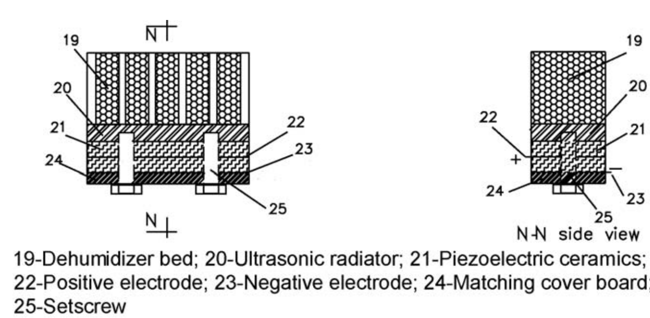


Fig. 18. Ultrasonic regenerator in the evaporative cooler. (19) Dehumidizer bed; (20) ultrasonic radiator; (21) piezoelectric ceramics; (22) positive electrode; (23) negative electrode; (24) matching cover board; (25) set screw.

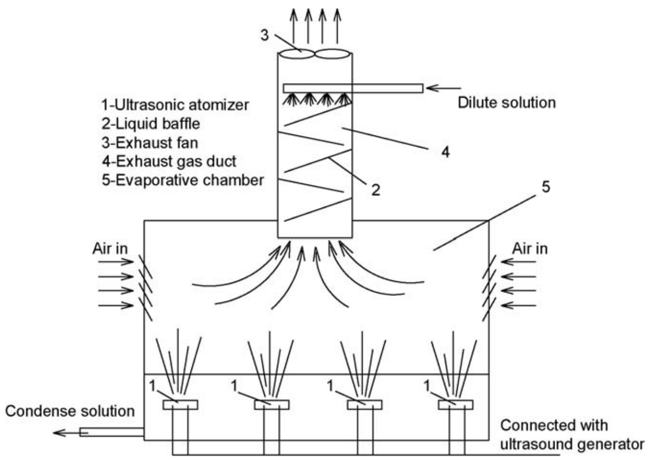


Fig. 19. Ultrasonic regenerator for liquid-desiccant system. (1) Ultrasonic atomizer; (2) liquid baffle; (3) exhaust fan; (4) exhaust gas duct; (5) evaporative chamber.

heated to a lower relative humidity (e.g. <40%), and the fresh air to be processed by the water droplets should be cooled to a higher relative humidity (e.g. >80%) before it enters into the desiccant bed. It is noted that to what degree the fresh air is heated or cooled mainly depends on the energy utilization efficiency of the whole system.

For the liquid-desiccant system, the schematic representation for ultrasonic regenerator is shown Fig. 19. The dilute solution is condensed (regenerated) mainly through the evaporation. The purpose of liquid baffle is to prevent the tiny liquid droplets being vented with the air flow. The dilute solution flows along the baffle with the help of gravity and flushes away the crystalloid solute settled on the baffle. To improve the evaporation rate, the inlet air is heated to a lower relative humidity (e.g. <50%). This regenerator may help to improve the energy efficiency of the liquid-desiccant system because the regeneration proceeds under non-heating condition and the regenerated desiccant does not need to be cooled before its reuse for the air dehumidification.

5. Related issues to further study

5.1. Insight into the effects of power ultrasound on the enhancement

An analysis of the literature aforementioned indicates that ultrasonic drying or regeneration in fact make use of the mechanical and physical phenomena induced by ultrasound to enhance the rate of mass transfer processes. For liquid desiccants, it is the 'cavitation effect' (caused by power ultrasound in liquid environment and produces atomization) that mainly contributes to the improvement of regeneration (or condensation). It is in fact spray drying, a process of transforming a dilute solution into a condensed one. One key point in this application is to control over the best size distribution of liquid droplets produced by ultrasonic atomizer since too small size of droplets are easily carried away by the passing air, and the larger size will decrease the evaporation rate. Further study is needed to make on the influential factors, e.g. solution concentration, liquid temperature as well as acoustic parameters like intensity and frequency that impact the droplet radius distribution. The effect of conditions of the carrying air (temperature, relative humidity, and velocity) on the evaporation rate of ultrasonic atomization should be investigated as well for the better operation of the new regeneration system, which can refer to literature [62] in which the effect of gas velocity on the evaporation rate of ultrasonic atomization was examined. Finally, the corresponding models for the spray evaporation ought to be established for better understanding of the process.

For solid desiccants, the mechanism of regeneration improvement by ultrasound has been admitted as the 'thermal effect' and 'mechanical effect' of power ultrasonic. The relative importance of the 'mechanical effect' to the 'thermal effect' in the regeneration enhancement may be greatly influenced by the moisture ratio of the desiccant stuff. According to Kardashev [63], the mechanism of acoustic drying of capillary-porous materials depends on the moisture content level. When the material is very wet (moisture ratio = 200–500%), the effect of an ultrasound field is mainly mechanical. When the material moisture ratio is not very high (10–70%), the effect of ultrasound is both mechanical and thermal. And when the material content is very low, the sound waves enhance only the moisture diffusivity due to ultrasonic thermal effect. However, little study has quantitatively investigated the specific percentage of contributions of the two effects to the enhancement. The quantitative study will help us better understand the mechanism of ultrasonic dehydration in the regeneration of solid desiccants. As we know, acoustic energy attenuation during the transmission ultimately results in temperature rise in medium, which is the main reason of the thermal effect of ultrasonic. Although the temperature rise in desiccant is sure to be favorable for the regeneration, it makes more sense to make use of mechanical effect of ultrasonic to improve this process (desiccant regeneration) from the perspective of energy utilization.

During the conversion from electrical power energy to ultrasound waves through the ultrasonic transducer, some energy loss will inevitably take place. The energy equation can be expressed as:

$$E_{\text{input}} = E_{\text{loss}} + E_{\text{ultra}} \tag{19}$$

where E_{input}, E_{loss} and E_{ultra} denote total input energy, energy loss and ultrasound energy. The energy loss, E_{loss}, will inevitably convert into heat that makes a temperature rise in ultrasonic transducer.

During the propagation of ultrasonic waves in medium, some part of ultrasonic energy will be absorbed by materials (E_{absorbed}), and the rest is in the form of mechanical energy ($E_{\text{mechanical}}$) that induces micro-oscillation effect. The energy equation can be written as:

$$E_{\text{ultra}} = E_{\text{absorbed}} + E_{\text{mechanical}} \tag{20}$$

Please note that the mechanical energy, $E_{\text{mechanical}}$, then will ultimately change into heat and make the medium temperature rise.

Let

$$\eta_{\text{ult}} = \frac{E_{\text{ultra}}}{E_{\text{input}}} \tag{21}$$

$$\eta_{\text{abs}} = \frac{E_{\text{absorbed}}}{E_{\text{ultra}}} \tag{22}$$

where η_{ult} is the working efficiency of ultrasonic transducer. η_{abs} is the absorption coefficient of ultrasonic energy by medium.

Thus, the effective mechanical energy converted from the total input energy can be expressed as:

$$E_{\text{mechanical}} = (1 - \eta_{\text{abs}})\eta_{\text{ult}}E_{\text{input}} \tag{23}$$

To achieve more mechanical energy ($E_{\text{mechanical}}$), η_{ult} should be as high as possible, and η_{abs} be as low as possible. η_{ult} is related to the structure of ultrasonic transducer as well as the ultrasonic power and frequency produced [64]. η_{abs} is related to the acoustic characteristics of medium (e.g. sound attenuation and impedance) and the frequency of ultrasound. In the future work, the two crucial parameters, i.e. η_{abs} and η_{ult}, are to be experimentally determined under different circumstances.

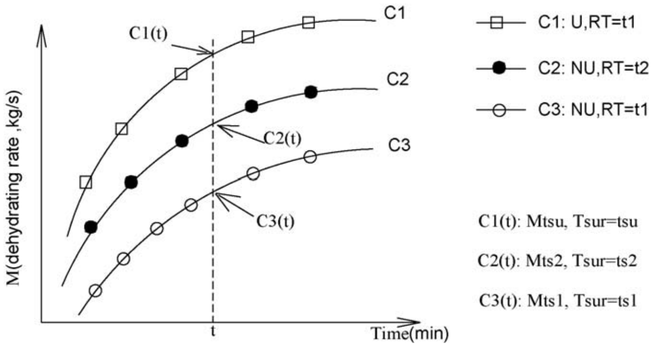


Fig. 20. Schematic representation for dehydrating curves under different conditions.

A preliminary idea is given as below for the quantitative estimation of ultrasonic 'thermal contribution' and 'mechanical contribution' to the improvement of desiccant regeneration.

The schematic curves of dehydration under different drying conditions are supposedly shown in Fig. 20. The curve marked with '□' (C1) corresponds to the drying conditions as follows: with ultrasonic radiation (U), $t1$ in the drying air temperature (RT); the curve with 'δ' (C2) to the conditions as follows: no ultrasonic radiation (NU), $t2$ in the drying air temperature (RT); and the curve with '○' (C3) has the following conditions: no ultrasonic radiation (NU), $t1$ in the drying air temperature (RT). The other conditions, e.g. the air flow rate and humidity, are the same for all the three cases.

It is reasonable to assume that the dehydration rate increase linearly with the surface temperature of desiccant under the same states of drying air. Taking the time point (t) as an example, the dehydrating rate under the conditions of C1, C2 and C3 is assumed, respectively, as 'Mtsu', 'Mts2' and 'Mts1'; and the corresponding surface temperature (Tsur) of desiccant is, respectively, as 'tsu', 'ts2' and 'ts1'. The percentage of ultrasonic 'thermal contribution' (η_t) and 'mechanical contribution' (η_m) to the regeneration improvement can be estimated, respectively, by Eqs. (24) and (25).

$$\eta_t\ (\%) = \left(\frac{\text{Mts2} - \text{Mts1}}{\text{Mtsu} - \text{Mts1}}\right) \cdot \left(\frac{\text{tsu} - \text{ts1}}{\text{ts2} - \text{ts1}}\right) \times 100 \tag{24}$$

$$\eta_m\ (\%) = (1 - \eta_t) \times 100 \tag{25}$$

The key parameter in the estimation of the separated contribution of ultrasonic effects is the surface temperature of desiccant (Tsur). It can be got by two ways: one is direct measuring, the other is calculating with the absorption coefficient of ultrasonic energy (η_{abs}) in medium based on the law of energy conservation.

5.2. Drying kinetics model for desiccant regeneration assisted by ultrasonic

Modeling of the drying processes is one of the most important aspects of drying technology for industrial processes, which can allow the engineers to choose the most appropriate method of drying as well as to choose suitable operating conditions. An analysis of the literature data indicates that acoustic drying in many cases becomes in fact sound-assisted convective drying, which is essentially similar in drying kinetics to conventional convective dying [65]. Generally, the drying models can be categorized as theoretical, semi-theoretical, and empirical models.

The most widely studied theoretical model in thin-layer drying is given by solution of Fick's second law. The Fick's law in spherical coordinates can be expressed as [66]:

$$\frac{\partial W}{\partial t} = \frac{\partial}{\partial r}\left(D_{\text{eff}} \frac{\partial W}{\partial r}\right) \tag{26}$$

where D_{eff} is effective water diffusivity (m^2/s). With the assumptions of moisture migration being by diffusion, negligible shrinkage, and constant diffusion as well as temperature, the solution of the Fick's second law for spherical geometry is given as follows [66]:

$$\frac{W_\tau - W_e}{W_0 - W_e} = \frac{6}{\pi^2} \sum_{n=1}^{\infty} \frac{1}{n^2} \exp\left[-\frac{n^2 \pi^2 D_{\text{eff}} \tau}{r_p^2}\right] \tag{27}$$

where W_τ is moisture ratio in material at any time (τ) of drying, kg/kg dry sample; W_0, W_e is initial and equilibrium moisture ratio, respectively. r_p is particle radius, m.

Drying of many food product, such as amaranth grain [67], wheat [68], chestnuts [69], hull-less seed pumpkin [70] and pistachio nuts [71] has been successfully modeled by using Fick's second law. And for the drying process assisted by power ultrasound, the Fick's law has been used as well by some researchers to model the drying kinetics and predict the mass diffusivity [57,72–74]. However, the analytical solution to the theoretic model is obtained under some assumptions, especially for the constant diffusion and temperature that is impossible in the drying process assisted by power ultrasound. Comparatively, the numerical method may be more appropriate for the solution although it may face some challenges, such as highly non-linear and intricately coupled by the dynamic system variables. In the future work, a study of numerical strategies is necessary to provide fast and accurate computations of the equations which govern the ultrasonic drying process.

As theoretical models are complex and cumbersome, the simple semi-empirical and empirical models are hence favored by many researchers. The semi-theoretical models generally derive from the mathematical model simplification and fitting the experimental drying data. The commonly used models include the Page (Eq. (28)), the Lewis (Eq. (29)), the Henderson and Pabis (Eq. (30)) the Logarithmic (Eq. (31)) and the Weibull (Eq. (32)).

$$\frac{W_\tau - W_e}{W_0 - W_e} = \exp(-Kt^n) \quad \text{Page model} \tag{28}$$

$$\frac{W_\tau - W_e}{W_0 - W_e} = \exp(-Kt) \quad \text{Lewis model} \tag{29}$$

$$\frac{W_\tau - W_e}{W_0 - W_e} = A\exp(-Kt) \quad \text{Henderson and Pabis model} \tag{30}$$

$$\frac{W_\tau - W_e}{W_0 - W_e} = A\exp(-Kt) + C \quad \text{Logarithmic model} \tag{31}$$

$$\frac{W_\tau - W_e}{W_0 - W_e} = \exp\left(-\left(\frac{t}{\beta}\right)^\alpha\right) \quad \text{Weibull model} \tag{32}$$

In Eqs. (28)–(32), the empirical constants, A, C, K, n, α, β, are obtained by fitting the experimental drying curves. Some of these semi-theoretical models have been used to model drying of different agricultural products [75–80].

Due to the lack of diffusion coefficient in the equations, the semi-theoretical models can only depict the rate of drying according to the changes of water content in materials and cannot reflect the drying phenomenon in nature. So is the same shortcoming with the empiric model (typically as Eq. (33) [58,81]) that derives directly from the relation between the moisture content and the time of drying, in which the fundamental aspect of drying process is neglected.

$$\frac{W_\tau - W_e}{W_0 - W_e} = a + b \cdot \tau + c\tau^2 \tag{33}$$

Summarizing the analysis above, the basic schemes for the model development in the future work are given as follows.

First, mathematical equations are established using the Fick's law and the basic principle of energy conservation according to the process of ultrasonic drying;

Secondly, the empirical models of mass diffusivity in desiccants of different sorts are obtained by fitting the analytical solution about the mathematical equations to the experimental data under different drying conditions (e.g. moisture ratio in material, drying air states including temperature, humidity and velocity, acoustic frequency and power employed).

Thirdly, numerical strategies are developed to provide fast and accurate computations of equations which govern the drying process assisted by power ultrasound. The numerical results are to be evaluated by the experiments.

5.3. Development of ultrasonic transducer

The regeneration of desiccant is a new domain for ultrasound application. So, the ultrasonic transducer should be specially developed in the future work for this purpose in order to achieve a better effect. For applications of power ultrasound, the crucial problems to be solved are related to the efficient generation and transmission of ultrasonic energy. In solid–gas systems, the challenges confronted mainly include the high impedance mismatch between the ultrasonic transducer and air, which makes the acoustic wave transmission difficult, and the high acoustic energy damping due to the air filled in the porous medium. These difficulties may be overcome by adequately designing of ultrasonic application system, e.g. the transducers developed for solid food dehydration are featured as good impedance matching with air, large amplitude of vibration, high directional radiation and high-power capacity as well as extensive radiating area [82]. Another key point in design of ultrasonic transducer is the mode of energy propagation. Sound energy can be propagated as longitudinal waves or transverse waves through which the particles in material vibrate perpendicularly to the direction of sound wave motion. Since the transverse waves require a relatively rigid medium in order to transmit their energy, the sound-assisted applications in gas and liquid environments are designed to accommodate longitudinal waves [83]. In addition, the acoustic frequency and power of transducer should be fully considered according to physical characteristics and mass load of desiccant used in the system.

5.4. Others

The possible generalization of a new technology to the practice mainly depends, to a large extent, on its environmental impact and economic benefit. For the environmental impact, the possible harm to human body done by high-intensity ultrasonic radiation must be seriously assessed. Exposure to ultrasound can be either through direct contact, a coupling medium, or the air (airborne ultrasound). Limits for exposure from each mode should be treated separately. In general, direct contact exposure to high intensities of liquid-borne ultrasound is not allowed. So, the limits for human exposure to airborne ultrasound are emphasized. In Grigor'eva's work, the author thought airborne ultrasound is considerably less hazardous to man in comparison with audible sound, and proposed 120 dB be adopted as an acceptable limit for the acoustic pressure for airborne ultrasound [84]. After 2 years, Acton [85] proposed a criterion below which auditory damage and/or subjective effects were unlikely to occur as a result of human exposure to airborne noise from industrial ultrasonic sources over a working day. He based his criterion on the belief that it is the high audible frequencies present in the noise from ultrasonic machines, and not the ultrasonic frequencies themselves, that are responsible for producing subjective effects. He extended this criterion to produce

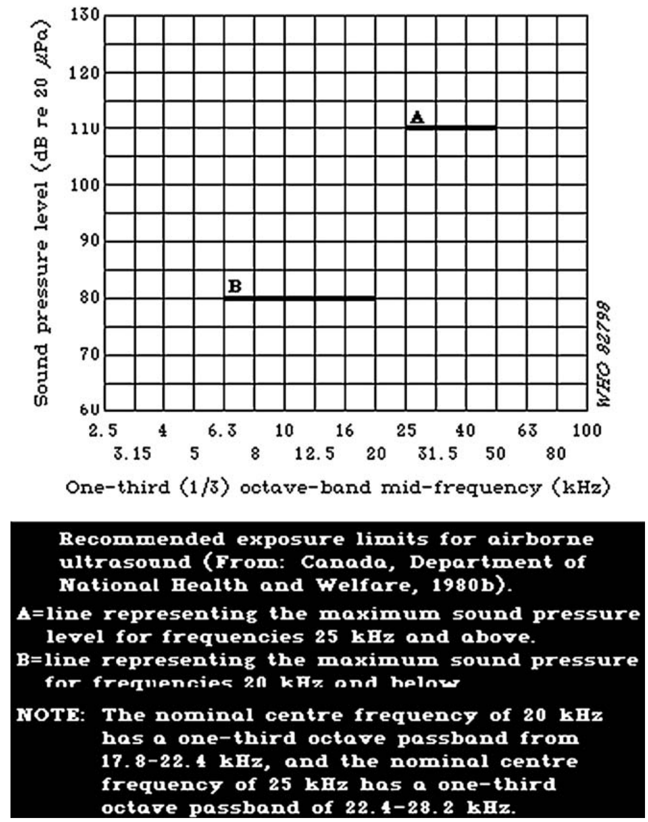


Fig. 21. Limits for human exposure to airborne acoustic energy issued by IRPA [88].

a tentative estimate for an extension to damage risk criteria, giving levels of 110 dB in the one-third octave bands centered on 20, 25, and 31.5 kHz. In his another paper published in 1974, Acton argued that additional data obtained for industrial exposures confirmed that the levels set in the proposed criterion were at approximately the right level, and that there did not seem to be any necessity to amend them [86]. The International Radiation Protection Association (IRPA) [87] has drafted the first international limits for human exposure to airborne acoustic energy having one-third octave bands with mid frequencies from 8 to 50 kHz, which is shown in Fig. 21 [88]. Measures should be taken to avoid the potential hazards caused by high-intensity ultrasound, e.g. persons exposed to high levels of noise associated with ultrasonic equipment should be protected either by wearing devices like earmuffs, or by acoustic barriers constructed around the equipment to reduce the noise levels.

The economic analysis for the new regeneration technology should be carefully made before it is applied in a desiccant system. Although it has been proved to be energy conservation [52] in experimental conditions, it is unknown in practical situations. Relevant energy simulation program should be developed to evaluate the potential energy-saving performance of the new regeneration method under different circumstances. In addition, an economic analysis model is needed to estimate the cost-recovery cycle of the added initial investment due to the additional equipments, i.e. the ultrasound generator and transducer.

6. Conclusions

A series of effects associated to power ultrasonic may increase the drying rate of moist material. In solid–gas system, the mass transfer enhancement caused by ultrasonic can be summarized by the two aspects: (1) increasing the solid-side moisture diffusivity due to ultrasonic thermal effect and/or mechanical effect; (2)

reducing the diffusion boundary layer through the oscillating velocities and micro-streaming at solid–gas interfaces induced by power ultrasonic. In liquid–gas system, the mass transfer enhancement caused by power ultrasonic can be explained as the increased area of liquid–gas interface because the liquid is atomized as numerous micron-size droplet and dispersed into the gaseous phase. The extensive review of recent literature related to ultrasonic dehydration indicates that most of these studies focused on the food drying applications, while only a small number of studies on the desiccant regeneration. Although the two field applications of power ultrasonic are similar and share most of the mechanisms, a lot of unexplored issues are still for further study on the ultrasonic applications in desiccant regeneration. These mainly include: (1) Insight into the effects of power ultrasonic on the enhancement of regeneration. It makes sense to have a quantitative investigation on the contributions of ultrasonic 'mechanical effect' and 'thermal effect' to the regeneration enhancement. (2) Modeling of the drying kinetics during the regeneration. It consists of a series of mathematical equations mainly based on the Fick's law, and proper numerical strategies. (3) Development of ultrasonic transducer special for this application. (4) Protection measures to reduce ultrasonic hazard to the environment.

Acknowledgements

This work was supported by the National Natural Science Foundation of China under contract no. 50708057 and the Specialized Research Fund for the Doctoral Program of Higher Education of China under contract no. 2007024811. Especially, the author will thank Professor Yanqing Chen (who is a professor at Mechanical Engineering Department of Purdue University) very much for his sincere help and support during the accomplishment of this review paper.

References

[1] Soleyn K. Humidity control: preventing moisture contamination. Chemical Engineering 2003;110(11):50–1.
[2] Chen XY, Jiang Y, Li Z, Qu KY. Field study on independent dehumidification air-conditioning system. I. Performance of liquid desiccant dehumidification system. ASHRAE Transactions 2005;111(2):271–6.
[3] Chen XY, Jiang Y, Li Z, Qu KY. Field study on independent dehumidification air-conditioning system. II. Performance of the whole system. ASHRAE Transactions 2005;111(2):277–84.
[4] Zhang LZ. Energy performance of independent air dehumidification systems with energy recovery measures. Energy 2006;31(8–9):1228–42.
[5] Cowie M, Liao XH, Radermacher R. Performance comparison of waste heat-driven desiccant systems. ASHRAE Transactions 2003;109(2):572–9.
[6] Techajunta S, Chirarattananon S, Exell RHB. Experiments in a solar simulator on solid desiccant regeneration and air dehumidification for air conditioning in a tropical humid climate. Renewable Energy 1999;17(4):549–68.
[7] Demakos PG. Improving IAQ with liquid-desiccant dehumidification. Heating/Piping/Air Conditioning HPAC Engineering 2009;81(9):36–42.
[8] Chang KS, Wang HC, Chung TW. Effect of regeneration conditions on the adsorption dehumidification process in packed silica gel beds. Applied Thermal Engineering 2004;24(5–6):735–42.
[9] Czanderna AW, Tillman NT, Herdt GC. Polymers as advanced materials for desiccant applications. Part 3. Alkali salts of PSSA and polyAMPSA and copolymers of polyAMPSASS. ASHRAE Transactions 1995;101(1):697–712.
[10] Jia CX, Wu JY, Wang RZ. Use of compound desiccant to develop high performance desiccant cooling system. International Journal of Refrigeration 2007;30(2):345–53.
[11] Yamamoto T, Tanioka G, Okubo M, Kuroki T. Water vapor desorption and adsorbent regeneration for air conditioning unit using pulsed corona plasma. Journal of Electrostatics 2007;65(4):221–7.
[12] Chakraborty M, Siva Kiran KT. Pressure swing adsorption: principles, processes and applications. Chemical Engineering World 2002;37(9):98–100.
[13] Azuara E, Garcıa HS, Beristain CI. Effect of the centrifugal force on osmotic dehydration of potatoes and apples. Food Research International 1996; 29(2):195–200.
[14] Rastogi NK, Eshtiaghi MN, Knorr D. Accelerated mass transfer during osmotic dehydration of high intensity electrical field pulse pretreated carrots. Journal of Food Science 1999;64(6):1020–3.
[15] Yao Y, Liu S. Ultrasonic—a new regeneration technology for dehumidizer. In: Wang RZ, Zhang P, editors. Proceedings of ICCR'2008 (The Fourth International Conference on Cryogenics and Refrigeration). Beijing: Science Press; 2008. p. 984–90.
[16] Breitbach M, Bathen D, Schmidt-Traub H. Desorption of a fixed-bed adsorber by ultrasound. Ultrasonics 2002;40(5):679–82.
[17] Hamdaoui O, Naffrechoux E, Tifouti L. Ultrasonic desorption of p-chlorophenol from granular activated carbon. Chemical Engineering Journal 2005;106(2): 153–61.
[18] Lim J, Okada M. Regeneration of granular activated carbon using ultrasound. Ultrasonics Sonochemistry 2005;12(4):277–82.
[19] Oualid H, Rabiaa D, Emmanuel N. Desorption of metal ions from activated carbon in the presence of ultrasound. Industrial and Engineering Chemistry Research 2005;44(13):4737–44.
[20] Juang RS, Lin SH, Cheng CH. Liquid-phase adsorption and desorption of phenol onto activated carbons with ultrasound. Ultrasonics Sonochemistry 2006;13(3):251–60.
[21] http://en.wikipedia.org/wiki/Ultrasound.
[22] Suslick KS. Ultrasound: its chemical, physical and biological effects. New York, USA: VCH Publishers; 1988.
[23] Kudra T, Mujumdar AS. Advanced drying technologies, 2nd ed., New York, USA: Taylor & Francis Group, LLC; 2009.
[24] Shutilov VA. Fundamental physics of ultrasound. Glasgow, UK: Bell and Bain Ltd.; 1988.
[25] Raj B, Rajendran V, Palanichamy P, editors. Science and technology of ultrasonics. UK: Alpha Science International Ltd.; 2004.
[26] Nagy PB. Slow wave propagation in air-filled permeable solids. Journal of Acoustical Society of America 1993;93(6):3224–34.
[27] Sun J, Besant RW. Heat and mass transfer during silica gel–moisture interactions. International Journal of Heat and Mass Transfer 2005;48(23–24): 4953–62.
[28] Kaeger J, Ruthven DM. Diffusion in zeolites and other microporous solids. New York, USA: Wiley; 1992.
[29] Edwards DK, Denny VE, Mills AF. Transfer processes, 2nd ed., New York, USA: Hemisphere/McGraw-Hill Book Company, Inc.; 1979.
[30] Pesaran AA. Moisture transport in silica gel particle beds. Ph.D. Dissertation. Los Angeles: School of Engineering and Applied Sciences, University of California; 1983.
[31] Rolando MA, Roque-Malherbe. Adsorption and diffusion in nanoporous materials. Taylor & Francis Group, FL, USA: CRC Press; 2007.
[32] Sladek KJ, Gilliland ER, Baddour RF. Diffusion on surface. II. Correlation of diffusivities of physically and chemically adsorbed species. Industrial & Engineering Chemistry fundamentals 1974;13(2):100–5.
[33] Pesaran AA, Mills AF. Moisture transport in silica gel packed beds. II. Experimental study. International Journal of Heat and Mass Transfer 1987;30(6):1051–60.
[34] Muralidhara HS, Ensminger D. Acoustic drying of green rice. Drying Technology 1986;4(1):137–43.
[35] Pesaran AA, Mills AF. Moisture transport in silica gel packed beds. I. Theoretical study. International Journal of Heat and Mass Transfer 1987;30(6): 1037–49.
[36] Fried E, Idelchik IE. Flow resistance: a design guide for engineers. New York, USA: Hemisphere Publishing Corporation; 1989.
[37] Lee CP, Wang TG. Outer acoustic streaming. Journal of the Acoustical Society of America 1990;88(5):2367–75.
[38] Hyun Sinjae, Lee Dong-Ryul, Byoung-Gook Loh. Investigation of convective heat transfer augmentation using acoustic streaming generated by ultrasonic vibrations. International Journal of Heat and Mass Transfer 2005;48(3–4):703–18.
[39] Yasuda K, Bando Y, Yamaguchi S, Nakamura M, Oda A, Kawase Y. Analysis of concentration characteristics in ultrasonic atomization by droplet diameter distribution. Ultrasonics Sonochemistry 2005;12(1):37–41.
[40] Clif R, Grace JR, Weber ME. Bubbles, drops and particles. Minneola, New York: Dover Publications, INC.; 2005.
[41] Jeong S, Garimella S. Falling-film and droplet mode heat and mass transfer in a horizontal tube LiBr/water absorber. International Journal of Heat and Mass Transfer 2002;45(7):1445–58.
[42] Gallego-Juarez JA, Rodriguez-Corral G, Galvez-Moraleda JC, Yang TS. A new high-intensity ultrasonic technology for food dehydration. Drying Technology 1999;17(3):597–608.
[43] Gallego-Juarez JA. Some applications of air-borne power ultrasound to food processing. In: Povey MJW, Mason TJ, editors. Ultrasound in food processing. Cornwall, UK: Blackie Academic & Professional; 1998.
[44] Mulet A, Carcel J, Benedito J, Rossello C, Simal S. Ultrasonic mass transfer enhancement in food processing. In: Jorge Welti-Chanes, Jorge F, Vélez-Ruiz, Gustavo V, Barbosa-Cánovas, editors. Transport phenomena in food processing. FL, USA: CRC Press LLC; 2003.
[45] Mulet A. Drying modelling and water diffusivity in carrots and potatoes. Journal of Food Engineering 1994;22(2):329–48.
[46] Carcia-Perez JV, Rossello C, Carcel JA, De la Fuente S, Mule A. Effect of air temperature on convective drying assisted by high power ultrasound. Defect and Diffusion Forum 2006;258–260:563–74.
[47] Yao Y, Liu S, Zhang W. Regeneration of silica gel using ultrasonic under low temperatures. Energy & Fuels 2009;23(1):457–63.
[48] Jakevicius L, Demcenko A. Ultrasound attenuation dependence on air temperature in closed chambers. Ultrasound 2008;63(1):18–22.
[49] Miclea C, Tanasoiu C, Amarande L, Miclea CF, Plavitu C, Cloangher M, Trupina L, et al. Effect of temperature on the main piezoelectric parameters of a soft PZT

ceramic. Romanian Journal of Information Science and Technology 2007;10(3):243–50.
[50] Garcia-Perez JV, Carcel JA, de la Fuente Blanco S, Riera-Franco de Sarabia E. Ultrasonic drying of foodstuff in a fluidized bed: parameteric study. Ultrasonics 2006;44(Suppl 1):e539–43.
[51] Garcia-Perez JV, Carcel JA, Benedito J, Mulet A. Power ultrasound mass transfer enhancement. I. Food drying. Transactions of IchemE Part C Food and Bioproducts Processing 2007;85(C3):247–54.
[52] Yao Y, Zhang W, Liu S. Feasibility study on power ultrasonic for regeneration of silica gel. Applied Energy 2009;86(11):2304–400.
[53] Sato M, Matsuura K, Fujii T. Ethanol separation from ethanol–water solution by ultrasonic atomization and its proposed mechanism based on parametric decay instability of capillary wave. Journal of Chemical Physics 2001;114(2):2382–6.
[54] Kirpalani DM, Toll F. Revealing the physicochemical mechanism for ultrasonic separation of alcohol–water mixtures. Journal of Chemical Physics 2002; 117(8):3874–7.
[55] Taylor SR, Hansen JC. Novel ultrasonic method for food hydration. Natick, MA, USA: Natick R, D&E Center [Natick/TR-94/014 (AD A277 411)], 1994.
[56] Garcia-Perez JV, Carcel JA, Riera E, Mulet A. Influence of the applied acoustic energy on the drying of carrots and lemon peel. Drying Technology 2009; 27(2):281–7.
[57] Yao Y, Zhang W, Liu S. Parametric study of high-intensity ultrasonic for silica gel regeneration. Energy &Fuels 2009;23(6):3150–8.
[58] Jambrak AR, Mason TJ, Paniwnyk L, Lelas V. Accelerated drying of button mushrooms, brussels sprouts and cauliflower by applying power ultrasound and its rehydration properties. Journal of Food Engineering 2007;81(1):88–97.
[59] Yao Y, Liu S, Chen J. Rotary desiccant dehumidifier assisted by high-intensity ultrasound. Chinese Patent, authorized number: ZL 200710173264.7; July 22, 2009.
[60] Jain S. Emulating nature: evaporative cooling system. ASHRAE Transactions 2008;114(2):421–7.
[61] Yao Y, Liu S, Chen J. Evaporative cooling air-conditioning system based on ultrasonic technology. Chinese Patent, authorized number: ZL 200710173263.2; May 20, 2009.
[62] Bando Y, Yamaguchi S, Doi K, Nakamura M, Yasuda K, Oda A, Kawase Y. The effect of operational condition on the contribution of evaporation in ultrasonic atomization. Journal of Chemical Engineering of Japan 2004;37(10):1286–9.
[63] Kardashev GA. Physical methods of process intensification in chemical technologies. Moscow: Khimiya; 1990, 208p [in Russian].
[64] Lin S, Zhang F. Measurement of ultrasonic power and electro-acoustic efficiency of high power transducers. Ultrasonics 2000;37(8):549–54.
[65] Kudra T, Mujumdar AS. Advanced drying technologies, 2nd ed., 2009.
[66] Crank J. The mathematics of diffusion. London, UK: Oxford University Press; 1975.
[67] Resio ANC, Aguerre RJ, Suarez C. Drying characteristics of amaranth grain. Journal of Food Engineering 2004;65(2):197–203.
[68] Gaston AL, Abalone RM, Giner SA, Bruce DM. Effect of modelling assumptions on the effective water diffusivity in wheat. Biosystems Engineering 2004; 88(2):175–85.
[69] Guine RPF, Fernandes RMC. Analysis of the drying kinetics of chestnuts. Journal of Food Engineering 2006;76(3):460–7.
[70] Sacilik K. Effect of drying methods on thin-layer drying characteristics of hull-less seed pumpkin. Journal of Food Engineering 2007;79(1):23–30.
[71] Kashaninejad M, Mortazavi A, Safekordi A, Tabil GL. Thin-layer drying characteristics and modeling of pistachio nuts. Journal of Food Engineering 2007;78(1):98–108.
[72] Garcia-perez JV, Carcel JA, Benedito J, Mulet A. Power ultrasound mass transfer enhancement in food drying. Trans IchemE Part C Food and Bioproducts Processing 2007;85(C3):247–54.
[73] Fabiano ANF, Sueli R. Ultrasound as pre-treatment for drying of fruits: dehydration of banana. Journal of Food Engineering 2007;82(2):261–7.
[74] Francisco Jr EL, Rodrigues Sueli. Ultrasound as pre-treatment for drying of pineapple. Ultrasonics Sonochemistry 2008;15(6):1049–54.
[75] Machado MD, Oliveira FAR, Cunha LM. Effect of milk fat and solid concentration on the kinetics of moisture uptake by ready-to-eat breakfast cereal. International Journal of Food Science and Technology 1999;34(1):47–57.
[76] Akpinar E, Midilli A, Bicer Y. Single layer drying behaviour of potato slices in a convective cyclone dryer and mathematical modeling. Energy Conversion and Management 2003;44(10):1689–705.
[77] Akpinar EK, Bicer Y, Cetinkaya F. Modeling of thin layer drying of parsley leaves in a convective dryer and under open sun. Journal of Food Engineering 2006;75(3):308–15.
[78] Gunhan T, Demir V, Hancioglu E, Hepbasli A. Mathematical modelling of drying of bay leaves. Energy Conversion and Management 2005;46(11–12):1667–79.
[79] Togrul IT, Pehlivan D. Modelling of thin layer drying kinetics of some fruits under open-air sun drying process. Journal of Food Engineering 2004; 65(4):413–25.
[80] Roberts JS, Kidd DR, Olga Padilla-Zakour. Drying kinetics of grape seeds. Journal of Food Engineering 2008;89(4):460–5.
[81] Panchariya PC, Popovic D, Sharma AL. Thin layer modelling of black tea drying process. Journal of Food Engineering 2002;62(3):63–72.
[82] Mulet A, Carcel JA, Sanjuan N, Bon J. New food drying technologies—use of ultrasound. Food Science and Technology International 2003;9(1):215–21.
[83] Bashford AG, Hutchins DA, Schindel DW. Radiated fields of an air-coupled ultrasonic capacitance transducer. Ultrasonics 1996;34(1):169–72.
[84] Grigor'eva VM. Effect of ultrasonic vibrations on personnel working with ultrasonic equipment. Soviet Physics—Acoustics 1966;11(3):426–7.
[85] Acton WI. A criterion for the prediction of auditory and subjective effects due to airborne noise from ultrasonic sources. Annals of Occupational Hygiene 1968;11:227–34.
[86] Acton WI. The effects of industrial airborne ultrasound on humans. Ultrasonics 1974;12(5):124–7.
[87] IRPA. Draft: Guidelines on limits of human exposure to airborne acoustic energy having one-third octave bands with mid frequencies from 8 to 50 kHz. International Radiation Protection Association, International Non-Ionizing Radiation Committee (IRPA/INIRC); November 1981.
[88] World Health Organization. International programme on chemical–environmental health criteria. 22: Ultrasound. Geneva, Switzerland; 1982.